HSYA inhibits Aβ1-42 -induced neuroinflammation by promoting microglial M2 polarization via TREM2/TLR4/NF- κB pathway in BV-2 cells.

Mengqiao Ren (873666849@qq.com)
Shihezi University
Mengyu Zhang
Shihezi University
Xiaoyan Zhang
Shihezi University
Chunhui Wang
Shihezi University
Yanjie Zheng
Shihezi University
Yan-li Hu
Shihezi University https://orcid.org/0000-0002-9811-5572

Research Article

Keywords: Hydroxysafflor yellow A, TREM2, Amyloid-β peptide, Neuroinflammation, Microglia

Posted Date: March 24th, 2021

DOI: https://doi.org/10.21203/rs.3.rs-336023/v1

Abstract

Hydroxysafflor yellow A (HSYA), an extract from *Carthamus tinctorius L*. Dry flowers (Compositae). HSYA has been shown to have neuroprotective effects in several AD models. However, the exact mechanisms of HSYA regulate neuroinflammation have still not been clarified. In this study, we investigated the mechanism by which HSYA regulates microglia activation and neuroinflammation via TREM2, and further clarified its underlying molecular mechanism. We silenced TREM2 in BV-2 cells and evaluated the expression of inflammatory markers (TNF-α, IL-1β, IL-4, IL-6, IL-10, and IL-13). The results showed that HSYA could up-regulate cell activity and improve the morphology of BV-2 cells injured by $A\beta_{1-42}$. HSYA up-regulated expression of M1 markers (iNOS, IL-1β, IL-6) and down-regulated expression of M2 markers (Arg-1, IL-4, IL-10, IL-13) by TREM2, and changed microglia from M1 pro-inflammatory phenotype to M2 anti-inflammatory phenotype. HSYA inhibited the activation of TLR4/ NF-κB transduction pathway induced by $A\beta_{1-42}$ by up-regulating TREM2, and regulated the transcription of inflammatory cytokines by downstream transcription factors NF-κB p65 and IκB-α. In conclusion, HSYA regulated microglial inflammatory phenotype by regulating microglial (M1/M2) polarization in $A\beta_{1-42}$-induced BV-2 cells which may be mediated through TREM2/TLR4/NF-κB pathway.

1. Introduction

Alzheimer's disease (AD) is a degenerative disease of the central nervous system. Its main clinical manifestations are progressive cognitive impairment and memory impairment(Reitz and Mayeux 2014). AD is characterized by brain atrophy and enlargement of the ventricles, accumulation of protein amyloid-beta plaques in the brain, and the presence of neurofibrillary tangles(Nestor et al. 2008; Bloom 2014). Numerous studies have shown that Aβ plays a dominant role in the occurrence and development of AD. According to the amyloid cascade hypothesis, the neurofibrillary tangles and neuroinflammation observed in AD are caused by Aβ accumulation(Kepp 2016).

Neurotoxic Aβ can activate astrocytes and microglia(Rogers et al. 1988). Microglia are the resident immune cells of the central nervous system and the first line of defense of the central nervous system(CNS)(Schafer et al. 2012). Once exogenous stimulation or microenvironment changes is felt, microglia can be activated to have the ability to deformation and phagocytosis. Microglia mediate multiple facets of neuroinflammation, which plays a double-edged role in various brain diseases via distinct microglial phenotypes. In different microenvironments, activated microglia can be polarized in M1 phenotype with host defense and pro-inflammatory functions and the M2 phenotype with neuroprotection, nerve repair, or neural ring remodeling functions(Zhou et al. 2014; Colton et al. 2006). Activated M1 microglia can release a large number of inflammatory cytotoxic mediators, including tumor necrosis factor-α (TNF-α), interleukin-1β (IL-1β), interleukin-6 (IL-6), and oxidative stress-related indicators such as reactive oxygen species (ROS), reactive nitrogen, and nitric oxide (NO). By contrast, the activated M2 microglia can increase the expression of anti-inflammatory mediators and neurotrophic factors, such as transforming growth factor-β, interleukin10 (IL-10), arginase-1 (Arg-1), and CD206(Dong et al. 2019; Subhramanyam et al. 2019). Therefore, inhibiting the overactivated

inflammatory microglia M1 phenotype by switching to the protective M2 phenotype appears to be a potential therapeutic strategy in neuroinflammatory disorders.

The activation process of Aβ on microglia is inseparable from the large number of Aβ receptors on the microglia membrane, such as Triggering Receptor Expressed on Myeloid Cells-2 (TREM2) and Toll-like receptors (TLR)(Beach et al. 2010). Several genetic variants of the TREM2 have been demonstrated to increase the risk of Alzheimer's disease (AD), thereby supporting the role of microglia and immune cells in AD(Guerreiro et al. 2013). TREM2 can regulate the function of microglia and transform its phenotype from M1 to M2. It can inhibit the release of inflammatory cytotoxic mediators and up-regulate the expression of anti-inflammatory factors, thereby reducing neuroinflammation damage to brain cells(Rohn 2013; Jonsson et al. 2013). TLR4/NF-κB and other signal molecules are the same as TREM2, which are critical to the modulation of microglial activation and neuroinflammation. TLR4 is mainly expressed in cerebral microglia. Stimulated by appropriate ligands, the NF-κB pathway is further activated to induce the transcription of pro-inflammatory cytokines, which play an important role in the activation of M1 microglia(Shi et al. 2019; Wan et al. 2016). Studies were confirmed that the TREM2 pathway and TLR4 pathway are mutually inhibited, that is, anti-inflammatory effect of TREM2 can antagonize the pro-inflammatory effect of TLR4(Rosciszewski et al. 2017).

Hydroxy safflower yellow A (HSYA), is the main active component of safflower. In recent years, HSYA has been found that a neuroprotective effect is related to various mechanisms, such as reducing inflammation, scavenging oxygen free radicals, and inhibiting apoptosis after ischemia-reperfusion(Keiko et al. 2010). Gene chips showed that HSYA can significantly inhibit the expression of inflammatory factors after cerebral ischemia(Liu et al. 2013). Other studies have reported that HSYA can inhibit the inflammatory response of microglia after oxygen-glucose deprivation and have neuroprotective effects(J. Li et al. 2013). HSYA can also inhibit the inflammatory induced by $A\beta_{1-42}$, play a neuroprotective effect and improve the learning, and memory ability of AD mice(Hou et al. 2020). More and more studies have been conducted on the pharmacological mechanism of HSYA, indicating that HSYA may be a multi-target drug candidate for the treatment of AD. However, whether HSYA inhibits the polarization of $A\beta_{1-42}$-induced microglial phenotype and promotes microglial polarization to M2 phenotype remains unclear. Moreover, the molecular mechanisms underlying HSYA-mediated anti-neuroinflammatory effects remain unknown.

In the current study, we aim to investigate whether the imbalance between TLR4 and TREM2 of microglia in $A\beta_{1-42}$-induced BV-2 cells mediates microglia polarization and neuroinflammation. We also analyzed the potential effects of HSYA on the polarization of microglia M1/M2. Our results may provide in-depth theoretical support for HSYA as a drug for the treatment of LOAD.

2. Materials And Methods

2.1 Materials and Microglia cells

HSYA (purity>98%) was purchased from Chengdu DeSiTe Biological Technology Co., Ltd. (Sichuan, China). The BV-2 mouse microglia cell line was purchased from Shanghai Fuheng Biological Co., Ltd. (Shanghai, China). $A\beta_{1-42}$ was purchased from Sigma-Aldrich(USA). $A\beta_{1-42}$HiLyte^{TM} Flour 647was purchased from ANASPEC PEPTIDE(USA). LV-TREM2 RNAi was purchased from Shanghai Genechem Co.,Ltd.(Shanghai, China). Enzyme-linked immunosorbent assay (ELISA) kits for TNF-α were acquired by Enzyme-Linked Biotechnology(China). Enzyme-linked immunosorbent assay (ELISA) kits for IL-1β, IL-4, IL-13, and antibodies to CD11b were purchased from Boster (China). PowerUp™ SYBR™ Green Master Mix and RevertAid First Strand cDNA Synthesis Kit were purchased from Thermo(USA). UNIQ-10 Column Trizol Total RNA Isolation Kit was acquired from Sangon Biotech(China). HRP-conjugated AffiniPure Goat Anti-Mouse IgG (H + L), HRP-conjugated Affinipure Goat Anti-Rabbit IgG(H + L), antibodies for IκB-α, p-IκB-α, NF-κB p65, and p-NF-κB p65 were supplied by Affinity (USA). Antibodies for TLR4 and Arg-1 were acquired from Santa Cruz Biotechnology(USA). Antibodies for TREM2 were purchased from Abcam(USA). Antibodies against beta-actin and goat anti-mouse AlexFluor488® were obtained from Zsbio(China). Goat anti-rabbit AlexFluor488® was obtained from Cell Signaling Technology(USA).

2.2 Preparation of $A\beta_{1-42}$ solutions

To generate soluble oligomers, $A\beta_{1-42}$ peptide was dissolved in 1,1,1,3,3,3-hexafluoro-2-propanol (HFIP; Sigma- Aldrich) at a concentration of 1 mM and then incubated for 24 hours under a fume hood(T. Jiang et al. 2014). The residual peptide film was dissolved to a concentration of 5 mM in dry dimethyl sulfoxide (DMSO). For oligomeric conditions, the peptide was dissolved in the peptide in a serum-free DMEM high glucose medium to a final concentration of 100 uM and kept at 4 °C for 24 hours.

2.3 Cell Culture and Treatment

Immortalized mouse BV-2 microglia were cultured in DMEM (Gibco, USA)high glucose medium with 0.1% penicillin-streptomycin (Gibco, USA) and 10% fetal bovine serum (Zhejiang Tianhang Biotechnology Co., Ltd., China) in a humidified atmosphere containing 5% CO_2 and 95% air at 37℃. The cells were sub-cultured for further passages when they reached 80% confluence and the culture medium were changed every two days. The cells in the logarithmic growth phase can be used in the experiment. Cells were pretreated with or without $A\beta_{1-42}$ for 24 hours and treated with various concentrations of HSYA (1, 2.5, 5, 10, and 20 μM) for 24 hours.

2.4 Cell Viability Assay and Morphological Analysis

BV-2 cell viability was assessed by the MTT assay using a 96-well culture plate. BV-2 cells were inoculated with $A\beta_{1-42}$ or treated with different concentrations of HSYA for 24 hours, and the appropriate concentration was selected for the follow-up experiment. Briefly, BV2 cells were seeded and pretreated with $A\beta_{1-42}$ for 24 hours and treated with different concentrations of HSYA.MTT (Soleibao, China) solution (20 μL) was added to each well. After incubation at 37 °C for four hours. The liquid was discarded and 200 μL DMSO were added to shake for 10 minutes. The absorbance at 570 nm was read on the enzyme

meter (Thermo, USA). For morphological analysis, the cells were imaged with the Zeiss inverted microscope (Axio observer A1, Zeiss, Germany) at 100× magnification.

2.5 Phagocytosis Assay

BV-2 cells were spread in a 6-well culture plate at a density of 1×10^6 per well. BV-2 cells were treated with different concentrations of HSYA (1, 2.5, 5, 10, and 20 μM) for 24 hours. 500 nM $A\beta_{1-42}$ HiLyteTM Flour 647 (AnaSpec, USA)was added to each well. After incubation at 37 °C for four hours, the cells were harvested and washed with phosphate-buffered saline (PBS). Light scattering characteristics of each sample (1×10^5 cells) were analyzed by FACSCanto analyzer (BD Biosciences, USA).

2.6 Lentivirus Transduction

The lentivirus encoded the TREM2 shRNA sequence 5'-AGCGGAATGGGAGCACAGTCA-3'. Lentivirus containing TREM2 shRNA (LV-shTREM2) at 1×10^8 TU/ml were purchased from Genechem (Shanghai, China). BV-2 cells were plated into a 6-well culture plate(5×10^4 cells/well) and incubated overnight. The TREM2 lentiviral particles were used to infect the cells at an MOI of 10. After 12 hours of lentiviral adsorption and infection, the transfected cells were screened by the complete culture medium of 2.5 μg/mL puromycin (Soleibao, China). The lentivirus transduction efficiency was observed by a fluorescence microscope and the expression levels of TREM2 were validated using Western blot.

2.7 Determination of cytokine levels by ELISA

Measure inflammatory factors such as TNF-α (Enzyme-Linked Biotechnology, China), IL-1β (Boster, China), IL-4 (Boster, China), IL-13 (Boster, China) released into the culture medium. NC and LV-shTREM2 BV-2 cells were inoculated into a 6-well culture plate(1×10^6 cells/well). The cells were incubated with $A\beta_{1-42}$ (1 μM) for 24 hours and treated with HSYA (5 μM) for 24 hours. The supernatant was collected and the concentrations were measured by ELISA according to the manufacturer's instructions. Optical density (OD) was measured at 450nm using a microplate reader (Thermo, USA)

2.8 Quantitative PCR (qPCR) Assay

Total RNA was extracted using the UNIQ-10 Column Trizol Total RNA Isolation kit (Sangon Biotech, China). According to the standard protocol, the isolated RNA was treated with PrimeScript™ RT reagent Kit with gDNA Eraser (TaKaRa Bio INC, China) to eliminate genomic DNA and reverse-transcribed into single-stranded cDNA. Specific primers (Sangon Biotech, China) were used to amplify target genes by using QuantiNova^{TM} SYBR Green PCR kit (Qiagen, Germany). The Rotor-Gene Q system (QIAGEN, Malaysia) for qPCR analysis. Reaction conditions: pre-denaturation 95 °C, 10 min; 95 °C, 10s, 60°C, 45s, 40 cycles. Each sample was analyzed in triplicate, and calculate the relative expression of mRNA after normalizing IL-6 and IL-10. By comparing the CT value of the target gene with that of GAPDH, the relative change of gene expression level was $2^{-\Delta\Delta Ct}$. All primer sequences used are listed in Table 1.

Table 1

Primers sequences used for qPCR.

Gene	Forward primer	Reverse primer
IL-6	5′-TTCTTGGGACTGATGCTGGTG-3′	5′-CACAACTCTTTTCTCATTTCCACGA -3′
IL-10	5′-TTACCTGGTAGAAGTGATGCCC-3′	5′-GACACCTTGGTCTTGGAGCTTA -3′
GAPDH	5′-AAGAGGGATGCTGCCCTTAC-3′	5′-CCATTTTGTCTACGGGACGA -3

2.1 Western blot Analysis

NC and LV-shTREM2 BV-2 cells were plated into a 6-well culture plate at a density of 1×10^6 per well and treated as mentioned above. Protein of TREM2 was extracted by membrane protein extraction kit (Sangon Biotech, China). Other cultured cells were lysed with RIPA buffer(Solarbio, China) supplemented with protease and phosphatase inhibitors, scraped off, the flasks, and collected for protein extraction. The lysates were incubated on ice for 30 min, centrifuged at 4 °C at 12000 rpm for 20 minutes, and the supernatant was collected. The protein concentration was determined using the protein analyzer Q5000 (Thermo, USA) and quantitatively denatured. Proteins were separated by sodium dodecyl sulfate-polyacrylamide gel electrophoresis (SDS-PAGE) and transferred to polyvinylidene fluoride (PVDF) membrane at 23 V. After blocking with 5% skim milk or BSA in TBS-T for one hour, the PVDF membranes were incubated overnight at 4°C with the following primary antibodies: rat monoclonal anti-TREM2 (1:1000, Abcam, USA), rabbit monoclonal anti-TLR4 (1:1000, Santa, USA), rabbit polyclonal anti-NF-κB (1:750, Affinity, USA), rabbit polyclonal anti-p-NF-κB p65 (1:750, Affinity, USA), rabbit polyclonal anti-IκB-α (1:750, Affinity, USA)rabbit polyclonal anti-p-IκB-α (1:750, Affinity, USA), mouse monoclonal anti-β-actin (1:1000, ZSGB-BIO, China). On the next day, the membrane was washed four times with TBS-T buffer for five minutes each time and incubated for 60 minutes with anti-rabbit or anti-mouse, horseradish peroxidase (HRP)-conjugated immunoglobulin G (IgG) secondary antibody diluted in TBS-T(1: 10000). Finally, the membranes were washed four times with TBS-T buffer for five minutes each time. The protein signals were detected with an enhanced chemiluminescence kit (Thermo Fisher Scientific, USA) and detected with EC3 Imaging System (Ultra-Violet Products Ltd., UK). Image-Pro Plus6.0 image processing software was used to quantitatively analyze the gray value of the signal.

2.9 Immunofluorescence Assay

NC and LV-shTREM2 BV-2 cells were plated onto glass coverslips in 24-well(1 × 105 cells/well) culture plate and treated as mentioned above. The cells were washed twice with PBS and fixed with 4% paraformaldehyde (Solarbio, China) for 10 minutes at room temperature(25~ 30 °C) followed by permeabilization with 0.3% Triton X-100 (Solarbio, China) for 20 minutes. Cells were then blocked with 5% goat serum (Solarbio, China) in PBS for 30 minutes followed by incubation with rabbit polyclonal anti-CD11b (1:50, Cell Signaling Technology, USA), mouse monoclonal anti-Arg-1 (1:50, Santa, USA), and rabbit polyclonal anti-iNOS (1:200, Cell Signaling Technology, USA) at 4°C overnight. The next day, the cells were washed three times with PBS-T and incubated with goat anti-rabbit AlexFluor488® (1:1000, Cell Signaling Technology, USA) or goat anti-mouse AlexFluor488® (1:50, Zsbio, China) at room temperature in the

dark for one hour. The cellular nuclei was counterstained with 1 mg/ml PI (Solarbio, China) for 10 minutes in the dark and mounted with 50% glycerol (Solarbio, China). Fluorescence images were acquired using a confocal laser(LSM510, Zeiss, Germany). The quantification of the fluorescence intensity was performed by analyzing the fluorescence images using the ImageJ software.

2.10 Statistical analysis

Statistical analysis was performed using SPSS software 22.0(IBM, Inc., Armonk, NY, USA). One-way analysis of variance (ANOVA) followed by the Tukey test was used to assess the statistical significance of differences between groups. The results are expressed as the mean ± standard error (SEM). $P<0.05$ was considered a significant difference. $P<0.05$ is considered statistically significant.

3. Results

3.1 Effects of HSYA on the viability of BV-2 cells induced by $A\beta_{1-42}$.

To determine whether HSYA influences the viability of BV-2 cells, an MTT assay was performed 24 hours after treatment with various concentrations of HSYA ranging from 1 μM to 20 μM. Results (Fig. 1a) showed that HSYA concentrations less than 10 μM did not induce any detectable cytotoxicity but decreased BV-2 cell viability and induced cytotoxicity at 20 μM concentration. Therefore, the concentration of HSYA 1 μM, 2.5 μM, 5 μM, and 10 μM was used in subsequent experiments. To select the appropriate $A\beta_{1-42}$ induction concentration, MTT assay was performed 24 h after induction with various concentrations of $A\beta_{1-42}$ ranging from 1 μM to 10 μM. Results (Fig. 1b) showed that $A\beta_{1-42}$ (1 μM, 5 μM, 10 μM) did decrease BV-2 cell viability and induced cytotoxicity. The viability of BV-2 cells was greatly inhibited and decreased by 30.26% when the concentration of $A\beta_{1-42}$ is 1 μM. Thus, the concentration of $A\beta_{1-42}$ 1 μM was used in subsequent experiments. BV-2 cells were incubated for 24 hours with or without $A\beta_{1-42}$ (1 μM) and treated with different concentrations of HSYA for 24 hours. Results (Fig. 1c) showed that HSYA at different concentrations (1 μM, 2.5 μM, 5 μM, and 10 μM) increased BV-2 cell viability compared with the $A\beta_{1-42}$ group. Results (Fig. 1d) of the morphological analysis showed that the resting microglia have good adhesion, normal shape, an elongated or oval cell bodies. From the cell body, elongated branch-like protrusions are rough and have spines. The nucleus is small and irregular in shape, with a kidney-shaped, oval, or triangular shape. However, the adherence of BV-2 cells induced by $A\beta_{1-42}$ is poor, and some cells can be observed floating in the medium under the microscope. Microglial cells present a typical activated state, showing rounding of the cell body and retraction of protrusions(Fig. 1e). Compared with the $A\beta_{1-42}$ group, the morphology of microglia in the HSYA treatment group was improved, that is, the increase of cell protrusions and the improvement of adherence(Fig. 1f). These results suggest that HSYA could reverse the decreased cell viability and morphological changes induced by $A\beta_{1-42}$.

3.2 HSYA has no obvious effect on phagocytosis of $A\beta_{1-42}$ by BV-2 cells

Abnormal accumulation of Aβ can activate microglia, and acute activation can promote the phagocytosis and clearance of Aβ by microglia, thereby exerting neuroprotective effects(Colton et al. 2006). Flow cytometry was used to detect the phagocytosis of $A\beta_{1-42}$ of BV-2 cells treated with different concentrations of HSYA. Compared with the control group, the phagocytosis of $A\beta_{1-42}$ of BV-2 cells in the HSYA treatment group was enhanced, but it was no significant change. (Fig. 2 a-b)

3.3 The effects of HSYA on the expression of TREM2 in BV-2 cells

TREM2 is a β-amyloid receptor that regulates the function of microglia. As showed in Fig. 3a-b, the western blot showed an upregulation of TREM2 expression in HSYA (5 μM) group and a significant downregulation of TREM2 expression in HSYA (10 μM) group compared with the control group. Therefore, the concentration of HSYA 5 μM was used in subsequent experiments

3.4 Effects of HSYA on the production of inflammatory cytokines in $A\beta_{1-42}$-induced BV-2 cells

Both ELISA and qRT-PCR were used to investigate whether HSYA regulated the expression of in- flammatory cytokines. The $A\beta_{1-42}$-induced production of TNF-α, IL-1β, IL-4, IL-13 was measured by ELISA, and IL-6, IL-10 was measured by qRT-PCR. Results (Fig. 4a-d) showed that the level of pro-inflammatory cytokines was greatly increased by $A\beta_{1-42}$ induction, as evidenced by the production of IL-1β. The anti-inflammatory cytokines (IL-4, IL-13) were decreased after $A\beta_{1-42}$ induction. Importantly, HSYA treatment inhibited $A\beta_{1-42}$-induced pro-inflammatory cytokine (IL-1β) synthesis whereas the production of anti-inflammatory cytokines (IL-4 and IL-13) was increased. When TREM2 is silenced, the levels of pro-inflammatory cytokines were increased more significantly by $A\beta_{1-42}$ induction, as evidenced by the production of IL-1β. The anti-inflammatory cytokines (IL-4, IL-13) were decreased more significantly after $A\beta_{1-42}$ induction. Interestingly, HSYA treatment does not have any significant effect on the expression of anti-inflammatory cytokines (IL-4 and IL-13) when TREM2 is silenced. Similar to the results of ELISA analysis, the qRT-PCR results showed that treatment with $A\beta_{1-42}$ significantly increased the level of pro-inflammatory cytokines (IL-6). HSYA treatment inhibited $A\beta_{1-42}$-induced pro-inflammatory cytokine (IL-6) synthesis whereas the production of anti-inflammatory cytokines (IL-10) was increased. HSYA treatment has no significant effect on the expression of pro-inflammatory cytokines (IL-6) when TREM2 is silenced. These results indicate that HSYA exhibits anti-inflammatory effects in $A\beta_{1-42}$-induced BV-2 cells, and the TREM2 protein plays an important role in this process.

3.5 HSYA promotes the polarization of M1 phenotype to M2 phenotype in BV-2 cells induced by $A\beta_{1-42}$ through TREM2

CD11b was used as the markers of microglia activation, iNOS was used as the markers of M1 polarization, while Arg-1 was employed as the marker of M2 polarization. To evaluate whether the neuroprotective effect of HSYA was associated with BV-2 cell polarization, we measured the expression of iNOS and Arg-1 via immunofluorescence assay to determine the effect of HSYA on phenotype switch in BV-2 cells. As showed in Fig. 5a–f, the protein

expression of CD11b and iNOS were markedly down-regulated and the protein expression of Arg-1 was markedly upregulated by HSYA treatment, compared with that of the $A\beta_{1-42}$-induced group. When TREM2 was silenced, the protein expression of CD11b and iNOS was unpregulated more significantly by $A\beta_{1-42}$ induction. Interestingly, HSYA treatment does not have any significant effect on the expression of iNOS and Arg-1 when TREM2 was silenced. These results indicate that HSYA promoted the polarization of M1 phenotype to M2 phenotype in BV-2 cells induced by $A\beta_{1-42}$ through TREM2.

3.6 Effects of HSYA on $A\beta_{1-42}$-induced TREM2/TLR4/NF-κB pathways

It has been reported both TLR4 and TREM2 are microglial membrane receptors that play an important role in signaling pathways mediating inflammation. Because $A\beta_{1-42}$ may induce neuroinflammation via interaction with microglial membrane receptors, we first determined the levels of two key regulators, TLR4 and TREM2, in $A\beta_{1-42}$-induced BV-2 cells. The results(Fig. 5a–c) demonstrated that in the $A\beta_{1-42}$-mediated AD model, the expression of the TLR4 and TREM2 was increased. However, HSYA treatment effectively inhibited TLR4 expression. Interestingly, when TREM2 was silenced, the protein expression of TLR4 was upregulated more significantly by $A\beta_{1-42}$ induction, and HSYA treatment has no significant effect. As shown in Fig. 6a, d-e, $A\beta_{1-42}$ stimulation resulted in the phosphorylation of IκB-α, and NF-κB p65 without affecting the expression of IκB-α and NF-κB p-65. However, HSYA treatment decreased the expression of p-IκB-α and p-NF-κB p65. At the same time, when TREM2 was silenced, the protein expression of phosphorylation of IκB-α, and NF-κB p65 were upregulated more significantly by $A\beta_{1-42}$ inducation. HSYA treatment has no significant effect on the expression of phosphorylation of IκB-α, and NF-κB p65 when TREM2 was silenced. Together, these results indicate that HSYA eliminates $A\beta_{1-42}$-induced TLR4 activation and downstream NF-κB activation through TREM2, which may probably contribute to the over- activation of microglia.

4. Discussion

Among the various hypotheses about the pathogenesis of AD, most people believe that Aβ deposition is the initial factor and a key link in the development of AD. When Aβ deposits abnormally in fibrous form, it will produce greater neurotoxicity. This may lead to DNA damage of brain neurons, changes in the regulation of apoptosis proteins, and down-regulation of neuroprotective gene expression levels, thereby inducing neuronal cell apoptosis and causing central nervous system damage(Curran et al. 2003; Kaltschmidt et al. 1999). Microglia in the early stage of neurodegeneration help to clear Aβ, but the ability of microglia to clear Aβ may decrease with age. In the advanced stage of AD, microglia increase the deposition of Aβ by releasing pro-inflammatory cytokines, forming a vicious circle, leading to severe central nervous system damage(Khoury et al. 2007). Hydroxysafflor yellow A (HSYA) is the active component with the highest content in safflower yellow. Studies have demonstrated that HSYA has neuroprotective effects in both an animal model of vascular dementia and an AD mouse model induced by $A\beta_{1-42}$(Sun et al. 2018; Suning et al. 2019). In this study, we adjusted TREM2 to reduce the imbalance of the

TLR4-mediated NF-κB signaling pathway to regulate the microglia M1/M2 polarization, thereby exploring anti-inflammatory properties of HSYA on $A\beta_{1-42}$-induced neuroinflammation.

Abnormal accumulation of Aβ can activate microglia, and acute activation can promote the phagocytosis and clearance of Aβ by microglia, thereby playing a neuroprotective effect. On the other hand, long-term chronic activation will cause microglia to release pro-inflammatory cytokines, causing inflammation, and then aggravating AD(Zhou et al. 2014). In this study, results of MTT and microscopic observation showed that BV-2 cells induced by $A\beta_{1-42}$ showed a typical activated state of microglia. The cell body changed from a spindle-shaped multi-protrusion state to a round shape, the light transmittance of the cells deteriorated, the adhesion was poor, and the cell survival rate declined significantly. After treatment with different concentrations of HSYA, the morphology of BV-2 cells was improved and the cell activity was increased substantially. It is suggested that HSYA can improve the microglia damage induced by $A\beta_{1-42}$. The results of flow cytometry showed that the phagocytosis of $A\beta_{1-42}$ of BV-2 cells was enhanced after the intervention of different concentrations of HSYA, but the difference was not statistically significant. Therefore, we can assume that the neuroprotective effect of HSYA is not mainly achieved by regulating the phagocytosis of microglia.

The microglia stimulated by Aβ can induce the synthesis and secretion of pro-inflammatory factors, including IL-1β, IL-6, TNF-α, IFN-γ, TGF-β, growth factors, chemokines, and macrophage inflammatory protein 1α, 1β, 2 and most homogenous CCL2/monocyte chemotactic protein 1, as well as reactive oxygen species and reactive nitrogen groups(Michelucci et al. 2009; Benarroch 2013). Inflammatory response promotes the accumulation and deposition of Aβ, which leads to neuronal loss and cognitive impairment, which in turn promote the development of AD(Kyrkanides et al. 2011). ELISA and qPCR results showed that after induction by $A\beta_{1-42}$, the expression of pro-inflammatory cytokines IL-1β and IL-6 in BV-2 cells was up-regulated, while the anti-inflammatory factors IL-4 and IL-13 were down-regulated. After HSYA intervention, the expression of IL-1β and IL-6 was significantly down-regulated, and the expression of IL-4, IL-10, and IL-13 was up-regulated. It is suggested that HSYA exerts a neuroprotective effect by up-regulating the expression of anti-inflammatory factors and down-regulating the expression of pro-inflammatory factors that mediate inflammation. TREM2 is a major anti-inflammatory receptor in vivo, which transmits activation signals by binding to DAP12 and inhibits the release of inflammatory mediators(Daws et al. 2001; Ford and McVicar 2009). In this study, using $A\beta_{1-42}$ inductions in the presence of TREM2 silence, the up-regulation of pro-inflammatory cytokine expression and the down-regulation of anti-inflammatory factor expression in BV-2 cells were more significant. The therapeutic effect of HSYA is useless in the absence of TREM2. The results indicate that TREM2 plays an indispensable role in HSYA regulating the expression of microglia inflammatory factors.

Microglia are highly plastic cells. Activated microglia can be divided into the classic pro-inflammatory M1 phenotype and immunosuppressive M2 phenotype. M1/M2 only represents two simplified models of an extreme inflammatory response(Gaikwad and Heneka 2013). In fact, after stimulation and activation, the polarization state of microglia changes dynamically between the M1 and M2 phenotypes, which has neurotoxic and neuroprotective effects, respectively. Thus, whether neuroinflammation has

beneficial or harmful effects on CNS may critically depend on the type of microglia activation. It is worth noting that timely transfer of the M1 phenotype of microglia to the M2 phenotype is a promising strategy. More and more studies have found that regulating the polarization of microglia M1/M2 can inhibit the harmful effects of inflammation, create a microenvironment conducive to the recovery of the central nervous system, and enhance neuroprotection(Yang et al. 2016; Xiong et al. 2015). Therefore, our research focus on the role of HSYA in the regulation of microglia polarization. Immunofluorescence results showed that Aβ can induce BV-2 cells to up-regulate the expression of CD11b and iNOS, that is, induce microglia to polarize to M1. HSYA treatment can reduce the excessive activation of microglia and up-regulate the expression of Arg-1, that is, induce the polarization of microglia from the M1 phenotype to the M2 phenotype. However, when TREM2 is silenced, the activation of microglia and M1 polarization induced by Aβ is more pronounced, indicating that TREM2 can regulate the function of microglia and convert them from M1 to M2. After treatment with HSYA under the condition of TREM2 silence, the polarization phenotype of BV-2 cells did not change significantly. Combined with the expression results of related inflammatory factors, we can conclude that Aβ stimulation will increase the level of pro-inflammatory mediators, and the lack of TREM2 will lead to the activation of microglia and increased M1 polarization, thereby increasing the release of inflammatory mediators, leading to more serious Inflammation. HSYA regulates the microglia induced by $A\beta_{1-42}$ through TREM2 and induces the conversion of microglia from M1 to M2. Down-regulates pro-inflammatory factors and up-regulates anti-inflammatory factors, reduces inflammation, and plays a neuroprotective effect.

It is reported that the deletion of TREM2 aggravates the pathological accumulation of Aβ in the brain, especially in the hippocampus(Rohn 2013). As a β-amyloid receptor, TREM2 can directly bind to Aβ oligomers to mediate the function of microglia. After binding to Aβ, TREM2 can activate the immunoproliferative function of microglia, allowing microglia to gather around Aβ plaques to clear Aβ(Condello et al. 2018). In this study, we used different concentrations of HSYA to interfere with BV-2 cells. The results showed that the HSYA concentration of 5μM can significantly up-regulate the expression of TREM2 in BV-2 cells. The expression of TREM2 protein in BV-2 cells was significantly increased after induction by $A\beta_{1-42}$, while the expression of TREM2 protein after HSYA treatment decreased compared with the model group(Walter et al. 2007). This is mainly because the microglia associated with amyloid plaques increase the expression of TREM2 to control inflammation, thereby reducing the transcription of inflammatory cytokines in microglia, and can also promote the phagocytosis of Aβ by microglia(Zhong et al. 2017). It has been shown that TREM2/ DAP12 can reduce the activation of microglia induced by LPS by negatively regulating JNK and NF-κB signaling pathways, thus reducing the release of inflammatory factors such as IL-1β, TNF-α, and IL-6(Z. Li et al. 2017). As a key transcription factor, NF-κB plays an important role in the expression of pro-inflammatory cytokines. Generally, inactivated NF-κB is located in the cytoplasm bound to the IκB inhibitor. The activation of inflammatory stimuli (such as LPS) strongly enhances the phosphorylation and proteasome degradation of IκB inhibitory proteins, leading to the release of NF-κB and nuclear translocation(Mi et al. 2019). In the PD mouse model induced by 1-methyl-4-phenyl-1,2,3,6-tetrahydropyridine, TREM2 can negatively regulate the inflammatory pathway mediated by TLR4, reduce the activation of microglia, and the release of inflammatory factors such as TNF-α and IL-1β,

so as to play a neuroprotective role(-. T. Jiang et al. 2017). The results of this study showed that the expression of TLR4 in BV-2 cells was significantly up-regulated after induction by $A\beta_{1-42}$, which further resulted in a significant increase in the expression of p-NF-κB p65 and p-IκB. After HSYA treatment, the expression of TLR4 in BV-2 cells was significantly down-regulated, thereby reducing the phosphorylation level of downstream NF-κB p65 and IκB. In the case of TREM2 silence, the expression of TLR4, p-NF-κBp65, and p-IκB-α in BV-2 cells was up-regulated more significantly after induction by $A\beta_{1-42}$. It is suggested that TREM2 plays an indispensable role in regulating the activation of the TLR4/NF-κB pathway induced by $A\beta_{1-42}$. However, with HSYA treatment in the case of TREM2 silence, the phosphorylation of TLR4, NF-κBp65, and IκB-α did not significantly improve. It is inferred from this that HSYA regulates the TLR4/NF-κB pathway induced by $A\beta_{1-42}$ through TREM2, blocks the signal transduction of this pathway, inhibits the release of inflammatory factors, and thus exerts a neuroprotective effect.

In conclusion, our research shows that HSYA can improve the microglia damage induced by $A\beta_{1-42}$ through TREM2, and regulate the polarization transition of microglia from M1 to M2. At the same time, HSYA inhibits the TLR4 /NF-κB transduction pathway by up-regulating TREM2 and regulates the transcription events of downstream transcription factors NF-κB p65 and IκB-α on inflammatory cytokines. Therefore, it can alleviate the chronic neuroinflammatory response induced by $A\beta_{1-42}$, reduce nerve damage, and play a neuroprotective effect, providing an opportunity for the study of HSYA to prevent and treat AD.

Declarations

Funding This research was supported by the National Natural Science Foundation of China [No.81960665].

Conflict of interest The authors declare that they have no conflict of interest.

Consent to participate All authors agree to participate

Consent for publication All authors agree to publish

Data availability Available upon request.

Authors' contribution

Mengqiao Ren and Yanli Hu conceived and designed research. Mengyu Zhang and Mengqiao Ren conducted experiments. Xiaoyan Zhang, Mengqiao Ren, and Yanjie Zheng analyzed data. Mengqiao Ren wrote the manuscript; Chunhui Wang and Yanli Hu revised the manuscript. All authors read and approved the manuscript for publication. The authors declare that all data were generated in-house and that no paper mill was used.

Acknowledgements

Thanks to the National Natural Science Foundation of China for its support.

References

1. Beach TG, Walker R, Mcgeer EG (2010) Patterns of gliosis in alzheimer's disease and aging cerebrum. Glia 2(6):420–436
2. Benarroch -EE (2013) - *Microglia: Multiple roles in surveillance, circuit shaping, and response to injury* (Vol. – 81, Vol. – 12)
3. Bloom GS (2014) Amyloid-β and Tau: The Trigger and Bullet in Alzheimer Disease Pathogenesis. Jama Neurol 71(4):505–508
4. Colton -CA, Mott -RT, Sharpe -H, Xu -Q, Nostrand -WEV, Vitek -MP (2006) - *Expression profiles for macrophage alternative activation genes in AD and in mouse models of AD* (Vol. – 3)
5. Condello -C, Yuan -P, Grutzendler -J (2018) - *Microglia-Mediated Neuroprotection, TREM2, and Alzheimer's Disease: Evidence From Optical Imaging* (Vol. – 83, Vol. – 4)
6. Curran BP, Murray HJ, O'Connor JJ (2003) A role for c-Jun N-terminal kinase in the inhibition of long-term potentiation by interleukin-1beta and long-term depression in the rat dentate gyrus in vitro. Neuroscience 118(2):347–357
7. Daws -MR, Lanier -LL, Seaman -WE, Ryan -JC (2001) - *Cloning and characterization of a novel mouse myeloid DAP12-associated receptor family* (Vol. – 31, Vol. – 3)
8. Dong Y, Li X, Cheng J, Hou L (2019) Drug Development for Alzheimer's Disease: Microglia Induced Neuroinflammation as a Target? *International Journal of Molecular Sciences*, *20*(3)
9. Ford -JW, McVicar -DW (2009) - *TREM and TREM-like receptors in inflammation and disease* (Vol. – 21, Vol. – 1)
10. Gaikwad SM, Heneka MT (2013) Studying M1 and M2 states in adult microglia. Methods Mol Biol 1041:185–197
11. Guerreiro -R, Wojtas -A, Bras -J, Carrasquillo -M, Rogaeva -E, Majounie -E et al (2013) - *TREM2 variants in Alzheimer's disease* (Vol. – 368, Vol. – 2)
12. Hou J, Wang C, Zhang M, Ren M, Hu Y (2020) Safflower Yellow Improves the Synaptic Structural Plasticity by Ameliorating the Disorder of Glutamate Circulation in Aβ1-42-induced AD Model Rats. *Neurochemical Research*(449)
13. Jiang -T, Wan -Y, Zhang -Y-D, Zhou -J-S, Gao -Q, Zhu -X-C et al (2017) - *TREM2 Overexpression has No Improvement on Neuropathology and Cognitive Impairment in Aging APPswe/PS1dE9 Mice* (Vol. – 54, Vol. – 2)
14. Jiang T, Yu JT, Zhu XC, Tan MS, Gu LZ, Zhang YD et al (2014) Triggering receptor expressed on myeloid cells 2 knockdown exacerbates aging-related neuroinflammation and cognitive deficiency in senescence-accelerated mouse prone 8 mice. Neurobiol Aging 35(6):1243–1251
15. Jonsson T, Stefansson H, Stacy SPD, Jonsdottir I, Stefansson K (2013) Variant of TREM2 associated with the risk of Alzheimer's disease. *New England Journal of Medicine*, *368*(2)

16. Kaltschmidt B, Uherek M, Volk B (1999) Inhibition of NF-kB potentiates amyloid beta-mediated neuronal apoptosis. *Proceedings of the National Academy of Ences of the United States of America, 96*(16), 9409–9414
17. Keiko O, Yasuhiro, Irino, Tomomi S et al (2010) P2Y12 receptor-mediated integrin-β1 activation regulates microglial process extension induced by ATP. *Glia*
18. Kepp KP (2016) Ten Challenges of the Amyloid Hypothesis of Alzheimer's Disease. Journal of Alzheimers Disease 55(2):1–11
19. Khoury -JE, Toft -M, Hickman -SE, Means -TK, Terada -K, Geula -C et al (2007) - *Ccr2 deficiency impairs microglial accumulation and accelerates progression of Alzheimer-like disease* (Vol. – 13, Vol. – 4)
20. Kyrkanides -S, Tallents -RH, Miller -J-NH, Olschowka -ME, Johnson -R, Yang -M et al (2011) - *Osteoarthritis accelerates and exacerbates Alzheimer's disease pathology in mice* (Vol. – 8)
21. Li J, Zhang S, Lu M, Chen Z, Chen C, Han L et al (2013) Hydroxysafflor yellow A suppresses inflammatory responses of BV2 microglia after oxygen-glucose deprivation. Neuroence Letters 535(Complete):51–56
22. Li Z, Zhen-Lian Z, Xinxiu L, Chunyan L, Pengfei M, Tingting W et al (2017) TREM2/DAP12 Complex Regulates Inflammatory Responses in Microglia via the JNK Signaling Pathway. Frontiers in Aging Neuroence 9:204-
23. Liu Y, Lian Z, Zhu H, Wang Y, Chen X (2013) A Systematic, Integrated Study on the Neuroprotective Effects of Hydroxysafflor Yellow A Revealed by 1H NMR-Based Metabonomics and the NF-κB Pathway. *Evidence-Based Complementray and Alternative Medicine,2013,(2013-4-22), 2013*(9), 147362
24. Mi EK, Pu RP, Ju YN, Jung I, Cho JH, Lee JS (2019) Anti-neuroinflammatory effects of galangin in LPS-stimulated BV-2 microglia through regulation of IL-1β production and the NF-κB signaling pathways. *Molecular & Cellular Biochemistry*
25. Michelucci A, Heurtaux T, Grandbarbe L, Morga E, Heuschling P (2009) Characterization of the microglial phenotype under specific pro-inflammatory and anti-inflammatory conditions: Effects of oligomeric and fibrillar amyloid-β. J Neuroimmunol 210(1–2):3–12
26. Nestor SM, Rupsingh R, Borrie M, Smith M, Accomazzi V, Wells JL et al (2008) Ventricular enlargement as a possible measure of Alzheimer's disease progression validated using the Alzheimer's disease neuroimaging initiative database. *Brain*
27. Reitz C, Mayeux R (2014) Alzheimer disease: Epidemiology, diagnostic criteria, risk factors and biomarkers. Biochem Pharmacol 88(4):640–651
28. Rogers J, Luber-Narod J, Styren SD, Civin WH (1988) Expression of immune system-associated antigens by cells of the human central nervous system: relationship to the pathology of Alzheimer's disease. Neurobiol Aging 9(4):339–349
29. Rohn TT (2013) The Triggering Receptor Expressed on Myeloid Cells 2: "TREM-ming" the Inflammatory Component Associated with Alzheimer's Disease. *Oxidative Medicine and Cellular Longevity, 2013*, 1–8

30. Rosciszewski G, Cadena V, Murta V, Lukin J, Villarreal A, Roger T et al (2017) Toll-Like Receptor 4 (TLR4) and Triggering Receptor Expressed on Myeloid Cells-2 (TREM-2) Activation Balance Astrocyte Polarization into a Proinflammatory Phenotype. *Molecular Neurobiology*
31. Schafer -DP, Lehrman -EK, Kautzman -AG, Koyama -R, Mardinly -AR, Yamasaki -R et al (2012) - *Microglia sculpt postnatal neural circuits in an activity and complement-dependent manner* (Vol. – 74, Vol. – 4)
32. Shi H, Wang XL, Quan HF, Yan L, Pei XY, Wang R et al (2019) Effects of Betaine on LPS-Stimulated Activation of Microglial M1/M2 Phenotypes by Suppressing TLR4/NF-κB Pathways in N9 Cells. *Molecules*, *24*(2)
33. Subhramanyam CS, Wang C, Hu Q, Dheen ST (2019) Microglia-mediated neuroinflammation in neurodegenerative diseases. *Seminars in Cell and Developmental Biology*, *94*
34. Sun Y, Xu DP, Qin Z, Wang PY, Hu BH, Yu JG et al (2018) Protective cerebrovascular effects of hydroxysafflor yellow A (HSYA) on ischemic stroke. Eur J Pharmacol 818:604–609
35. Suning C, Mao S, Xianghui, Zhao et al (2019) Neuroprotection of hydroxysafflor yellow A in experimental cerebral ischemia/reperfusion injury via metabolic inhibition of phenylalanine and mitochondrial biogenesis. *Molecular Medicine Reports*
36. Walter -S, Letiembre -M, Liu -Y, Heine -H, Penke -B, Hao -W et al (2007) - *Role of the toll-like receptor 4 in neuroinflammation in Alzheimer's disease* (Vol. – 20, Vol. – 6)
37. Wan J, Shan Y, Fan Y, Fan C, Chen S, Sun J et al (2016) NF-κB inhibition attenuates LPS-induced TLR4 activation in monocyte cells. *Molecular Medicine Reports*
38. Xiong -X, Xu -L, Wei -L, White -RE, Ouyang -Y-B, Giffard -RG (2015) - *IL-4 Is Required for Sex Differences in Vulnerability to Focal Ischemia in Mice* (Vol. – 46, Vol. – 8)
39. Yang -J, Ding -S, Huang -W, Hu -J, Huang -S, Zhang -Y et al (2016) - *Interleukin-4 Ameliorates the Functional Recovery of Intracerebral Hemorrhage Through the Alternative Activation of Microglia/Macrophage* (Vol. – 10)
40. Zhong -L, Chen -X-F, Wang -T, Wang -Z, Liao -C, Wang -Z et al (2017) - *Soluble TREM2 induces inflammatory responses and enhances microglial survival* (Vol. – 214, Vol. – 3)
41. Zhou D, Huang C, Lin Z, Zhan S, Kong L, Fang C et al (2014) Macrophage polarization and function with emphasis on the evolving roles of coordinated regulation of cellular signaling pathways. Cell Signal 26(2):192–197

Figures

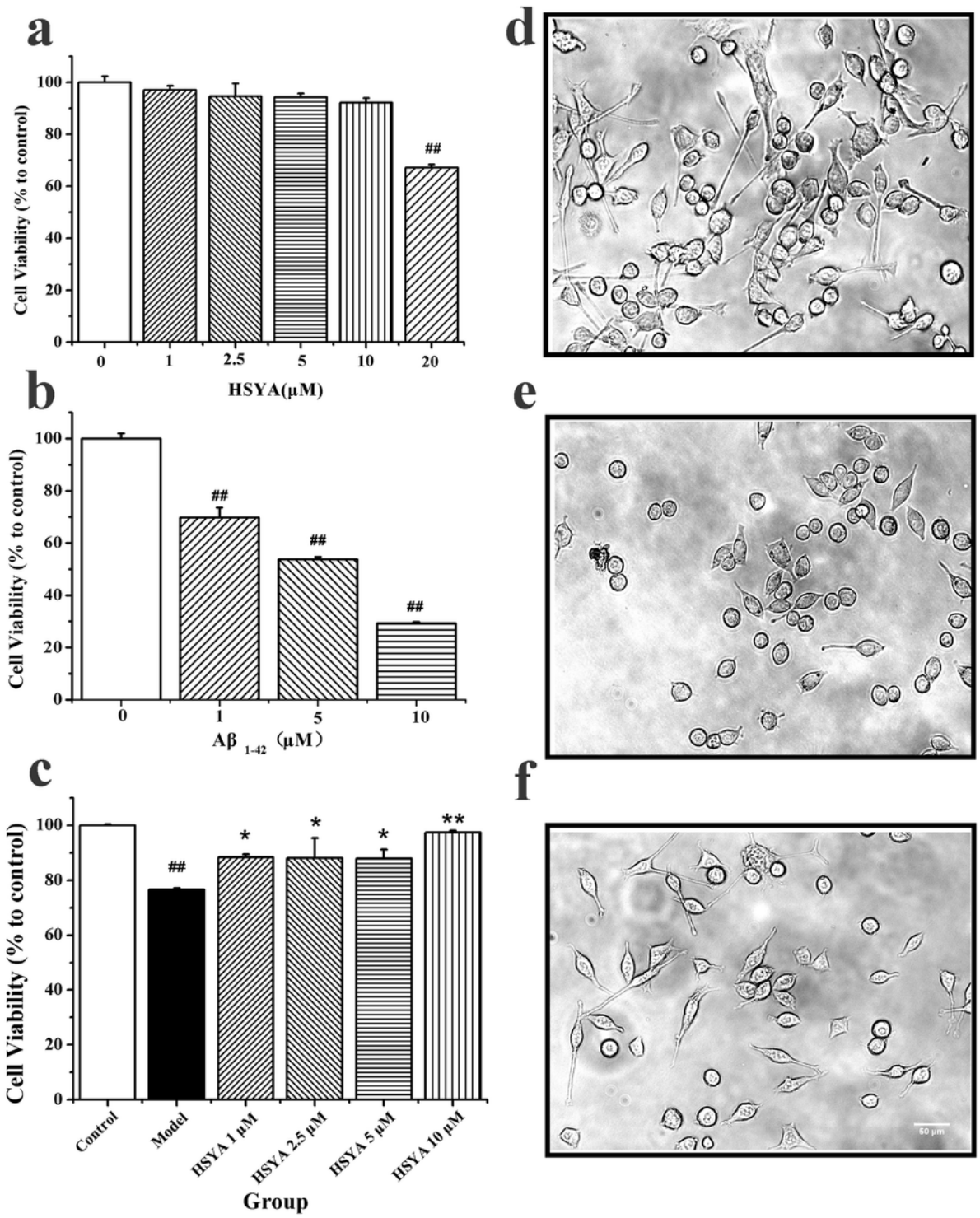

Figure 1

Effects of HSYA on the viability and morphology of BV-2 cells with or without Aβ1-42 inducation.a Effects of different concentrations of HSYA alone on cell viability b Effects of different concentrations of Aβ1-42 alone on cell viability c Effects of HSYA on cell viability induced by Aβ1-42. Cell morphology was observed with an optical microscope(200 x): d Control group; e Model group (Aβ1-42); f. HSYA group. Data are

represented as the mean ± S.E.M. (n=3).##p<0.01 versus control; *p<0.05,**p<0.01 versus model group. Scale bar = 50 μm

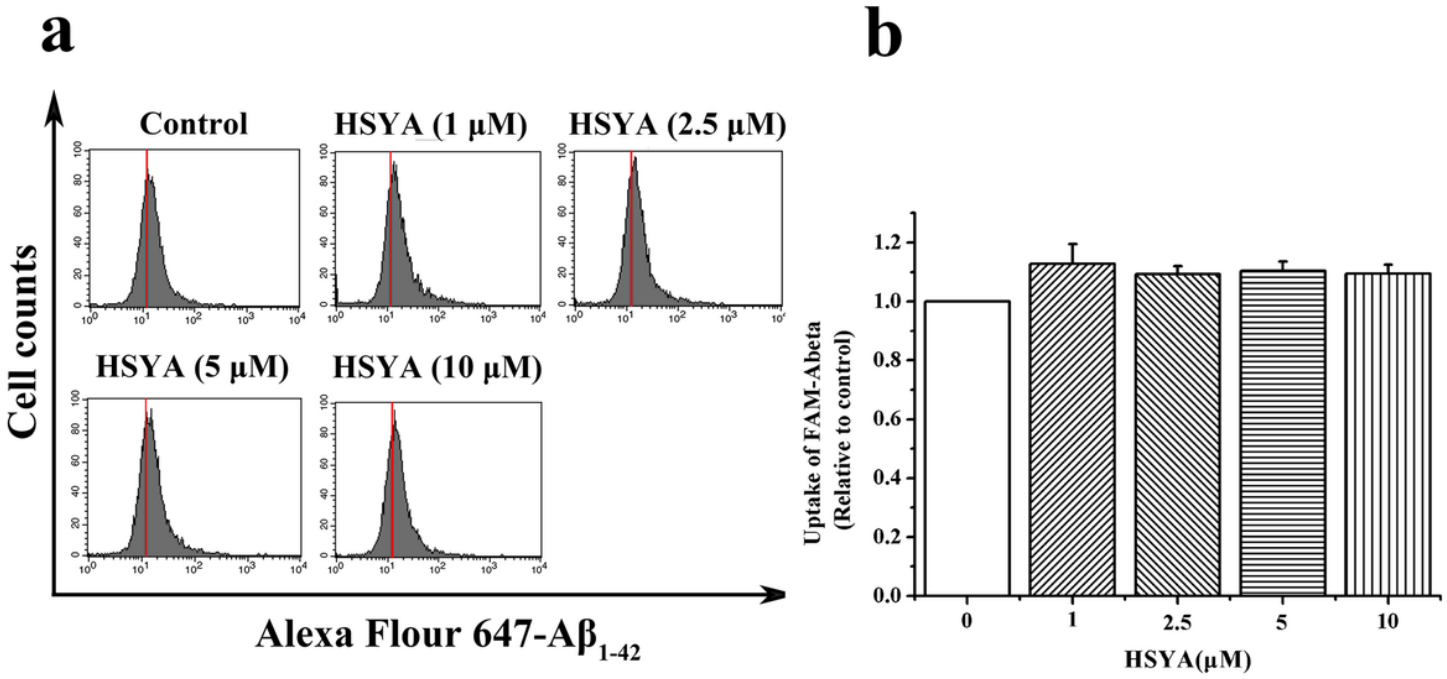

Figure 2

Effects of HSYA on Aβ1-42 phagocytosis of BV-2 cell by flow cytometry. BV-2 cells were treated with different concentrations of HSYA for 24 hours and treated with Aβ1-42 HiLyteTM Flour 647 for four hours a Peak diagram; b Statistical diagram of average fluorescence intensity. Data are presented as the mean ± S.E.M. (n=3).

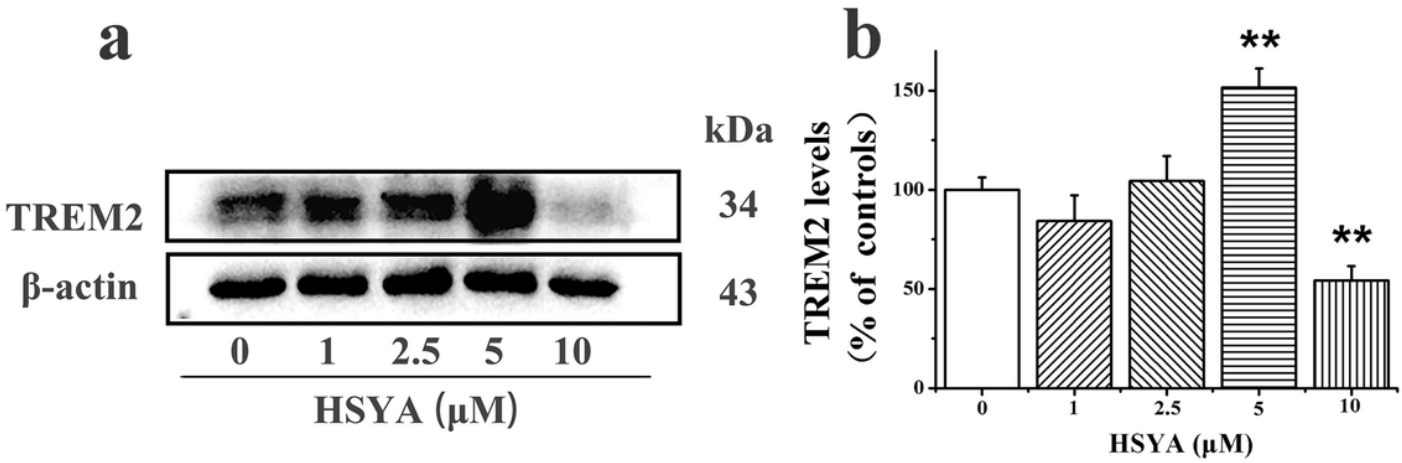

Figure 3

Effects of HSYA on the expression of TREM2 in BV-2 cells. Cells were treated with different concentrations of HSYA for 24 hours. Cultures were harvested to determine the protein expression of TREM2 via western

blot analysis. a Representative of TREM2 protein levels by western blot analysis. b The levels of TREM2. The results are represented as the mean ± S.E.M. (n=3~4). **P<0.01 versus control group.

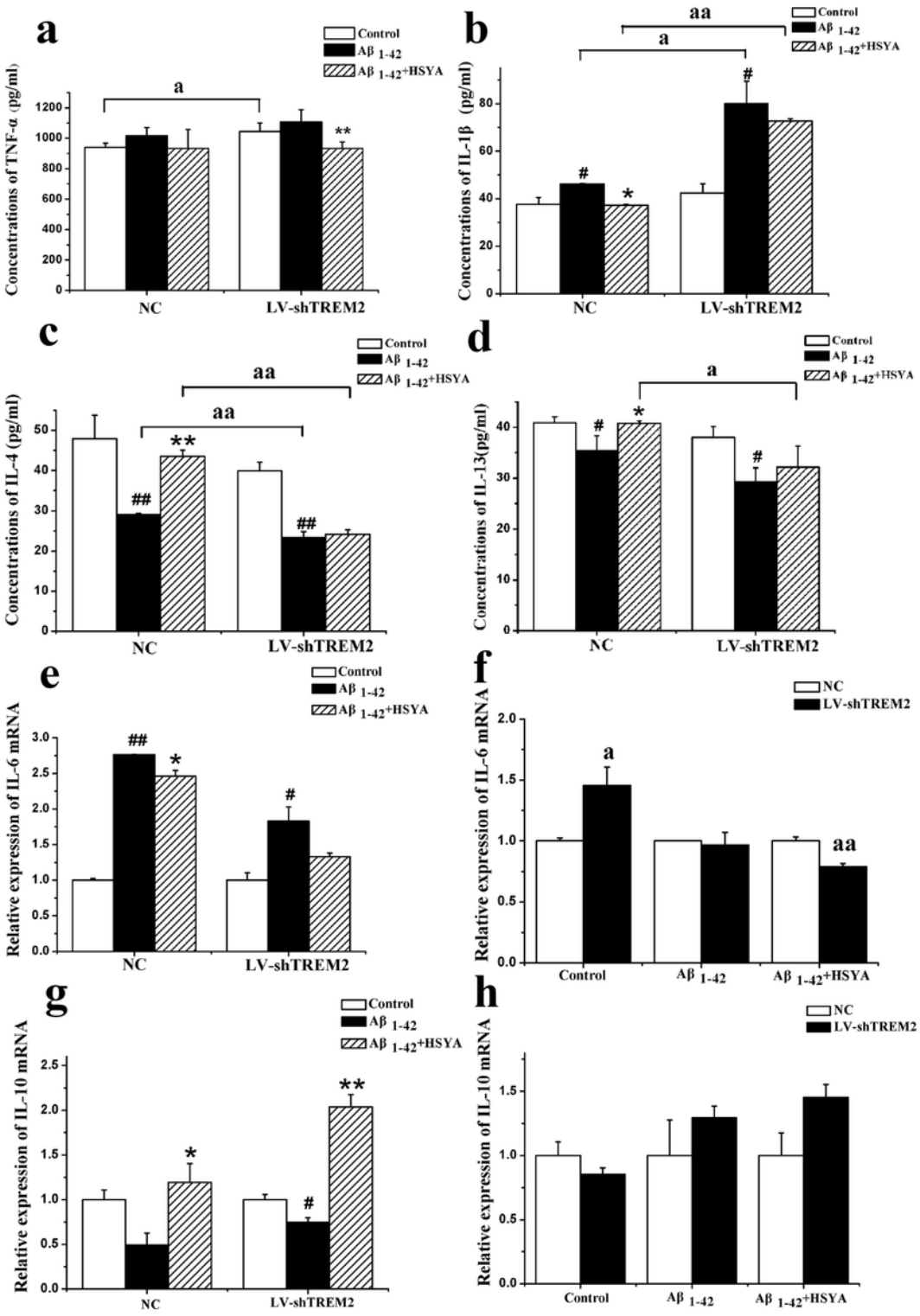

Figure 4

Effects of HSYA on the expression of inflammatory cytokines in BV-2 cells induced by Aβ1-42. NC and LV-shTREM2 BV-2 cells were incubated with Aβ1-42 (1 μM) for 24 hours and treated with HSYA(5 μM) for 24 hours. The expression of TNF-α (a), IL-1β (b), IL-4 (c), IL-13 (d) was detected by ELISA.The expression of

IL-6 (e-f), IL-10 (g-h) was detected by qPCR. Data are represented as the mean ± S.E.M. (n=3~4); ##P<0.01, #P<0.05 versus respective control group, **P<0.01, *P<0.05 versus respective model group; aaP<0.01, aP<0.05 versus NC at the same experimental condition.

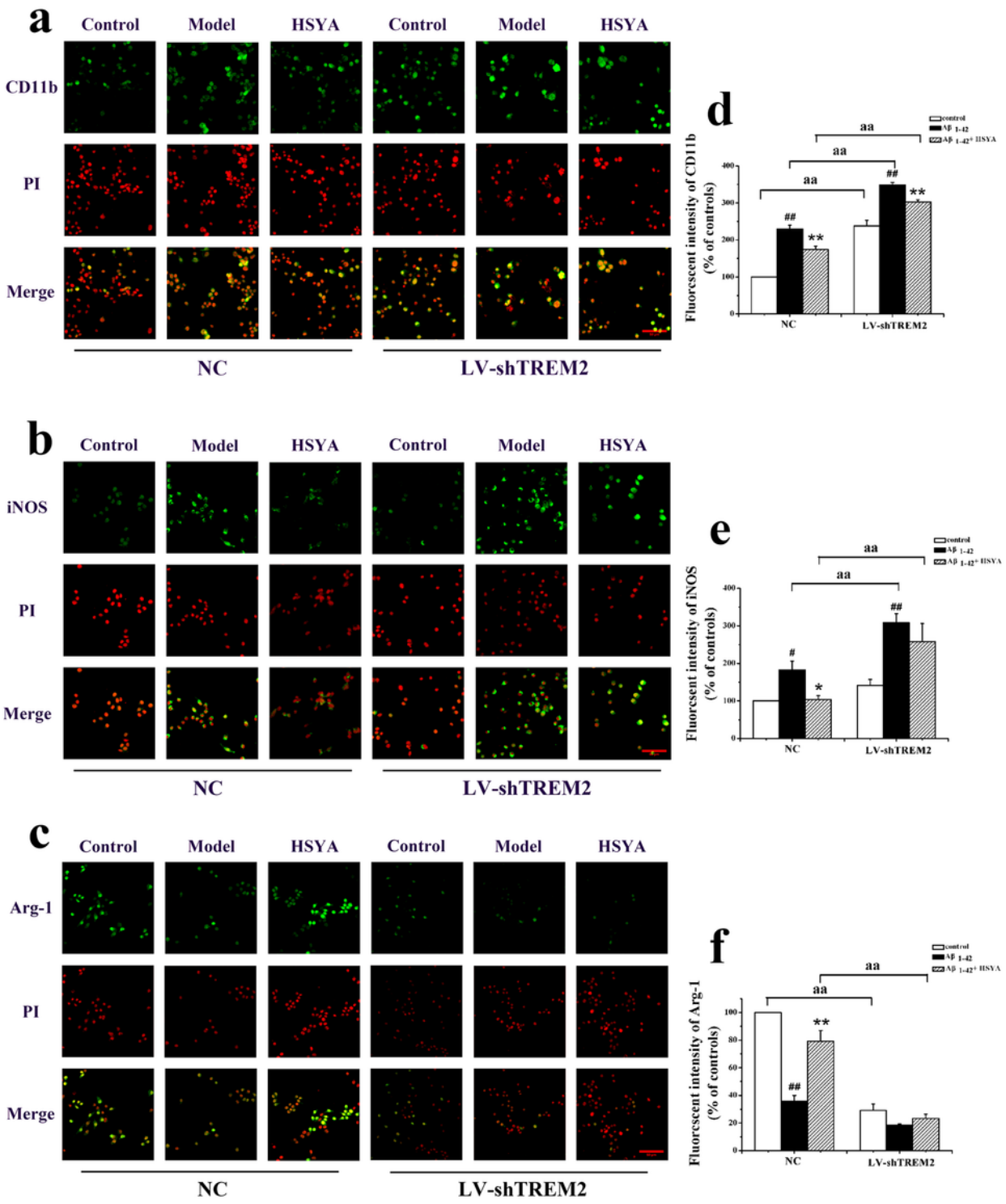

Figure 5

Effects of HSYA switched microglial polarization from M1 to M2 in Aβ1-42-induced BV-2 cells detected by immunofluorescence (200×). NC and LV-shTREM2 BV-2 cells were incubated with Aβ1-42 (1 μM) for 24

hours and treated with HSYA(5 μM) for 24 hours. a Cultures were visualized via immunostaining with anti-CD11b (green). b Cultures were visualized via immunostaining with anti-iNOS (M1 marker, green). c Cultures were visualized via immunostaining with anti-Arg-1 (M2 marker, green). Nuclei were stained with PI (red). Representative images of fluorescence intensity of CD11b(d), iNOS(e) and Arg-1(f). Data are represented as the mean ± S.E.M. (n=3); ##P<0.01, #P<0.05 versus respective control group, **P<0.01, *P<0.05 versus respective model group; aaP<0.01, aP <0.05 versus NC at the same experimental condition. Scale bar = 50 μm

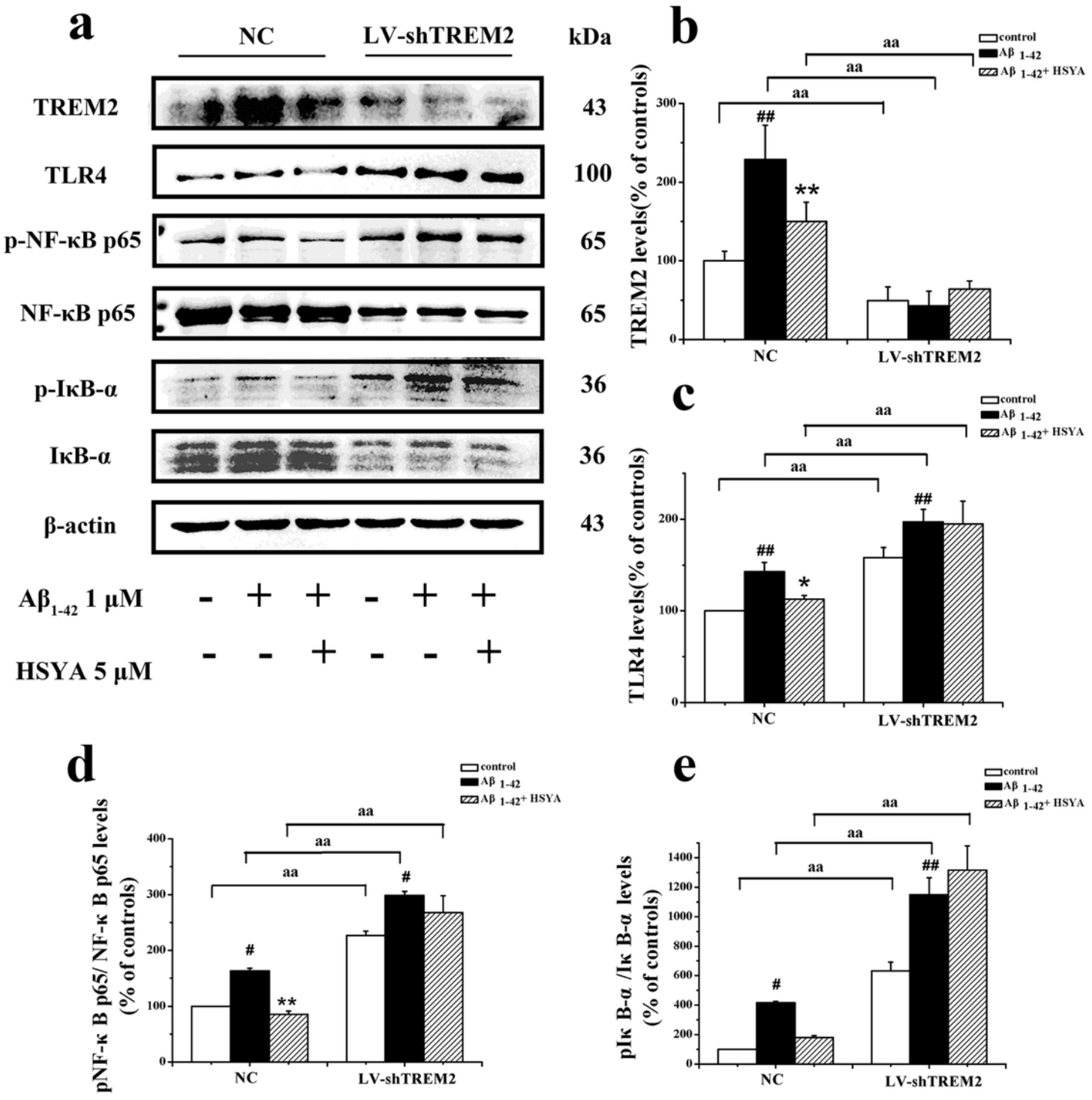

Figure 6

Effects of HSYA on Aβ1-42-induced TREM2/TLR4/NF-κB signal transduction in BV-2 cells. NC and LV-shTREM2 BV-2 cells were incubated with Aβ1-42 (1 μM) for 24 hours and treated with HSYA(5 μM) for 24 hours.The pathway-related proteins such as TREM2, TLR4, p-NF-κB p65, NF-κB p65, p-IκB-α, IκB-α were detected by Western blotting.a Representative western blots of TREM2, TLR4, p-NF-κB p65, NF-κB p65, p-IκB-α, IκB-α. b The levels of TREM2. c The levels of TLR4. d The levels of p-NF-κB p65/NF-κB p65. f The levels of p-IκB-α/IκB-α. Data are presented as the mean ± S.E.M. (n=3~4); ##P<0.01, #P<0.05 versus respective control group, **P<0.01, *P<0.05 versus respective model group; aaP<0.01, aP<0.05 versus NC at the same experimental condition.

Supplementary Files

This is a list of supplementary files associated with this preprint. Click to download.

- Data.pdf